CHAPTER 6 PERFORMANCE ASSESSMENT

Performance assessment of a structure under severe ground motions is commonly carried out using nonlinear static and nonlinear dynamic analyses (pushover and time-history analyses). These two methods present engineering demand parameters such as base shear and story drift response of the structure. However, collapse evaluation is not typically carried out. An alternative performance assessment method which evaluates probabilistic collapse capacity of the structure is recently presented in FEMA P695 (2009).

In this research, the collapse evaluation of the archetype structure was performed. The collapse evaluation was conducted according to FEMA P695 methodology. The analysis results are presented in terms of fragility curves, assuming log-normal cumulative distribution function (CDF). Performance sensitivity analysis was also carried out to investigate the effects of BRB ductility on the response of the structure.

A 2-D analytical model was created to represent the frame as described in Chapter 4. In summary, the model included P-Δ effect, "gravity" columns and the force-deformation characteristics of the columns and truss members following ASCE 41 (2006) recommendations. For the columns, a collapse criterion corresponding to a plastic rotation limit of 7% was assigned. This rotation limit was used as an indication for the onset of collapse. The force-deformation characteristics of the BRBs were calibrated based on existing test results (Merritt et al., 2003b). A core strain limit of 4% was assigned for the BRBs. The fracture of the BRBs was modelled by a sudden strength drop with only a minimal residual strength. It is important to note that the loss of one or a small number of BRBs does not necessarily mean that the loss of gravity load carrying capability of that collapse would occur. However, it does lead to significant increase in the deformation of the columns. In these analyses, the collapse was deemed to have occurred mainly when the plastic rotation of a column or top chord of the truss reached the limit. All of the analyses were carried out using PERFORM 3D computer program (CSI, 2007).

6.1 Nonlinear Static and Dynamic Analyses

Nonlinear static and nonlinear dynamic analyses were done to verify the response of a BRKB-TMF designed by the PBPD concept.

6.1.1 Nonlinear Static Analysis (Pushover)

The pushover analysis was done to determine the overall response, the sequence of inelastic activity leading to collapse, and the failure mechanism. Pushover was performed by applying increasing lateral loads. Lateral forces were defined corresponding to the distribution given by Equation (2-5). Figure 6.1 shows base shear versus roof drift plot. The graph indicates that the structure remained elastic until 0.5% drift. First yielding occurred in the BRBs at the load slightly beyond the design base shear (V/W= 0.154). The top chords and the columns started to yield at 1.4% and 1.6% drift, respectively. The peak strength occurred at the story drift of 1.9%. P-Δ effect became apparent beyond this drift level as can be seen from the gradual strength reduction. At 3.6% drift, a set of BRBs fractured and the frame experienced severe strength drop. Beyond this drift, the frame had only a modest lateral load resistance. As the loading continued, the plastic rotations of columns at the bases and the plastic

rotations of the truss top chords finally reached the rotation limit. It is apparent form the pushover results that the fracture of the BRBs signifies the impending collapse of the frame. It is therefore crucial to select the target drift that is compatible with deformation capacity of the BRBs. Overall, it can be seen that the presented PBPD procedure results in the frame that had all the inelastic activities confined to only the designated elements.

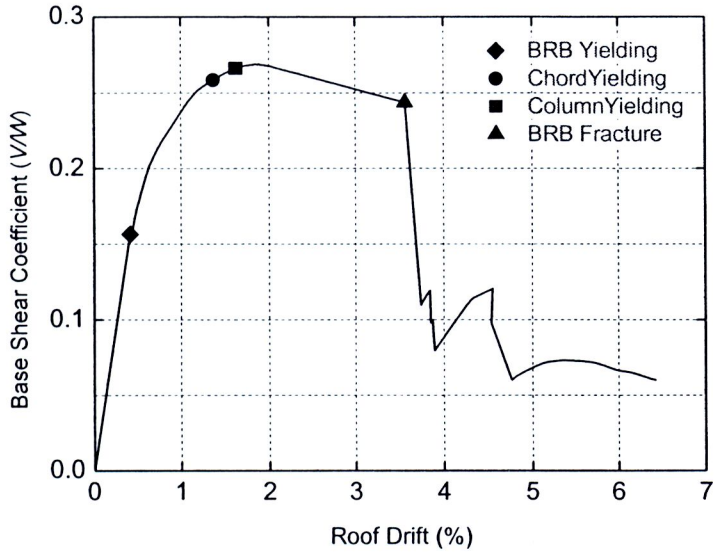

Figure 6.1 Pushover Curve of BRKB-TMF under PBPD Lateral Force Distribution

Pushover result was used to determine the overstrength factor (Ω) and period-based ductility (μ_T) according to FEMA P695 methodology (FEMA, 2009). The overstrength factor of the archetype structure was computed (Figure 6.2) as $\Omega = 0.269/0.154 = 1.75$. From Equation (2-12) $\delta_{y,eff}$ was 0.0054 and period-based ductility can be computed as $\mu_T = 0.036/0.0054 = 6.67$.

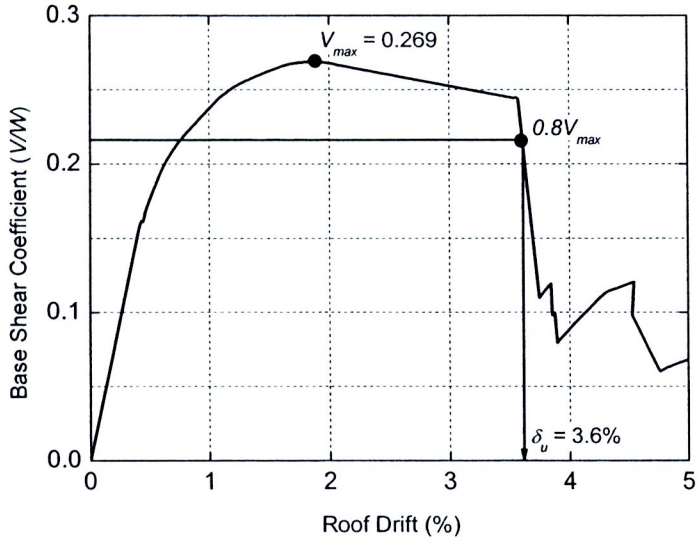

Figure 6.2 Overstrength and Period-Based Ductility Determined from Static Pushover Curve

The static overstrength factor (Ω) of the structure was 1.75, which was similar to the overstrength factor used in the design of the truss. This corresponds to a PBPD concept that the non-DYMs are designed to resist the applied force against DYMs with overstrength.

Figure 6.3 shows column moments from pushover analysis and PBPD column tree analysis when the structure reached maximum base shear. It can be seen that pushover moments of both exterior and interior columns were similar to the values according to column tree concept except for at the bases. The difference requires further study to improve the column tree analysis method.

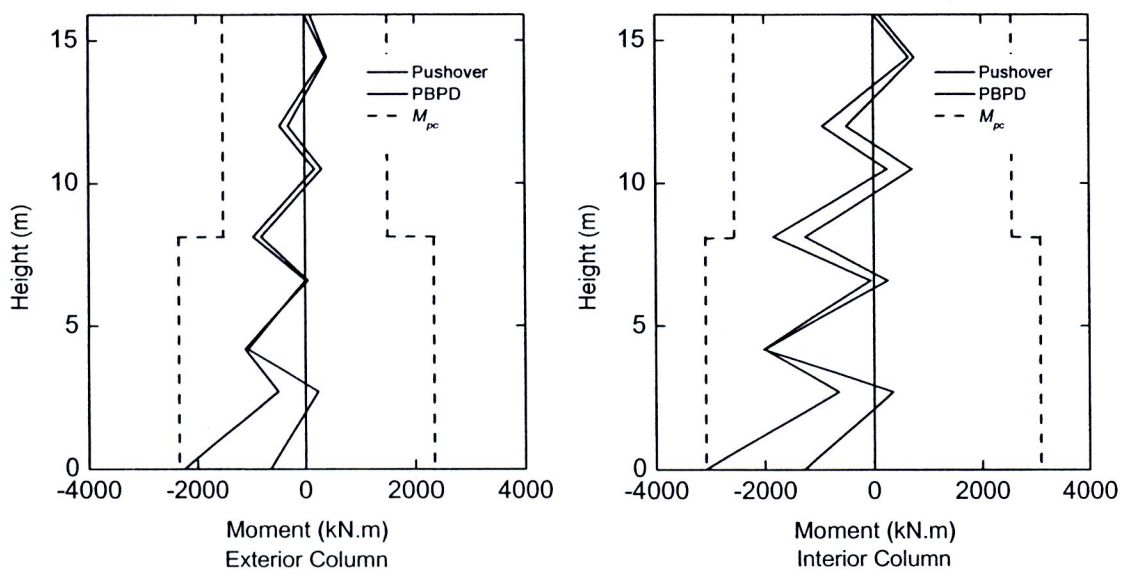

Figure 6.3 Column Moments at Maximum Base Shear

6.1.2 Nonlinear Dynamic Analysis (Time-History)

For nonlinear dynamic analyses, 44 ground motions representing the MCE and 2/3MCE levels were used. The ground motions were scaled such that their median spectral acceleration of the fundamental period matched with the design spectral acceleration at MCE and 2/3MCE levels. Under these 2 intensity levels, maximum interstory drifts of are illustrated in Figures 6.4 and 6.5.

Figure 6.4 shows maximum interstory drifts under 44 ground motions at 2/3MCE (0.64g) intensity level. As can be seen, the median value is lower than the design target drift of 2%.

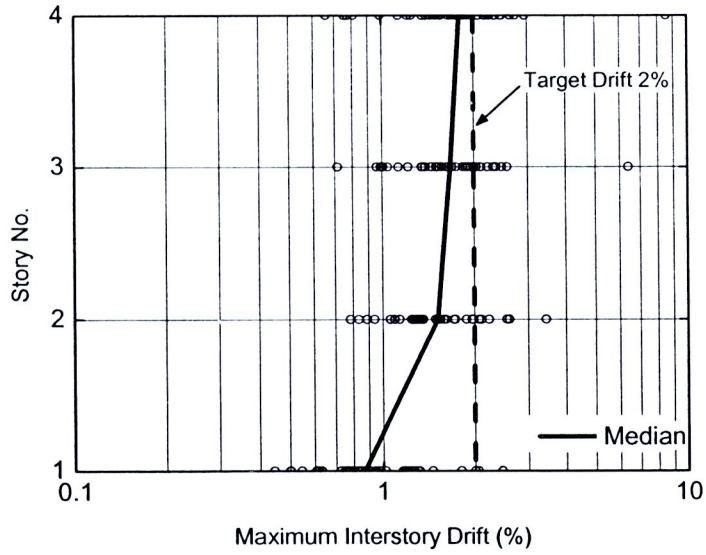

Figure 6.4 Maximum Interstory Drifts under 2/3MCE Ground Motions

Figure 6.5 shows maximum interstory drifts under 39 ground motions at MCE (0.96g) intensity level, excluding 5 ground motions that caused collapse of the archetype structure. As can be seen, the median value is lower than the design target drift of 3%.

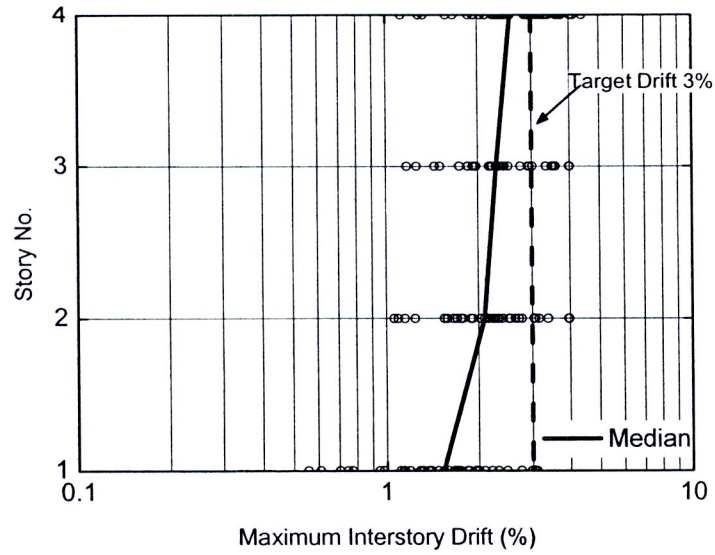

Figure 6.5 Maximum Interstory Drifts under MCE Ground Motions (excluding 5 collapse motions)

6.2 Collapse Evaluation

The results from the IDA are shown in Figure 6.6. One of the goals of FEMA P95 methodology is to assess the collapse capacity of the frame. The collapse capacity is expressed in terms of the collapse margin ratio (*CMR*) which is defined as the ratio between the median spectral acceleration of the collapse level ground motion (S_{CT}) and the spectral acceleration of the MCE ground motions (S_{MT}). From IDA results, the *CMR* for the example frame was found to be 1.56. The adjusted collapse margin ratio (*ACMR*) taking into account the spectral shape (FEMA, 2009) was computed and found to be 2.19.

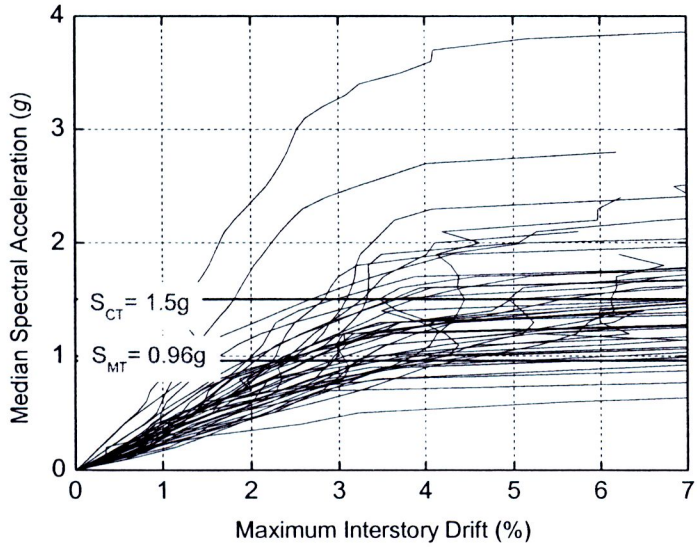

Figure 6.6 Incremental Dynamic Analysis Plotted between Intensity Measure (S_a) and Engineering Demand Parameter (θ)

SSF and *ACMR* of the archetype structure are summarized in Table 6.1 along with those of special concentrically braced frames (SCBF) and buckling restrained braced frames (BRBF) evaluated by Chen and Mahin (2010). The results of all structures were performed in the same seismic design category (SDC) D_{max}. As can be seen, the *CMR* and *ACMR* values are comparable to other structural systems with similar heights

Table 6.1 *CMR* and *ACMR* of SCBF, BRBF (Chen and Mahin, 2010) and BRKB-TMF

Archetype	SCBF[1]	SCBF[1]	BRBF[2]	BRBF[2]	BRKB-TMF
No. of Story	3	6	3	6	4
SDC	D_{max}	D_{max}	D_{max}	D_{max}	D_{max}
Static Ω	1.41	1.34	1.48	1.47	1.75
CMR	1.6	1.64	4.63	3.29	1.56
μ_T	6.1	6.6	22.7	15.5	6.67
SSF	1.28	1.36	1.39	1.53	1.41
ACMR	2.05	2.23	6.64	5.03	2.2

The *ACMR* value of BRKB-TMF was similar to that of SCBF but was lower than that of BRBF. This may be due to the large BRBs deformation demand. The fracture of the

BRBs when the core strain of BRBs reached maximum value was directly included in the modelling process.

To determine the allowable $ACMR_{20\%}$ (FEMA, 2009) for the BRKB-TMF, the total system collapse uncertainty (β_{TOT}) of the structure including assessment of uncertainties due to record-to-record variability, quality of test data, quality of design requirements, and quality of the analytical model are needed. Table 6.2 shows the total system collapse uncertainty (β_{TOT}) and the allowable $ACMR_{20\%}$ for a combination of good and fair quality of modelling, test data, and design requirement.

Table 6.2 Acceptable Values of Adjusted Collapse Margin Ratio

Quality			Total system Collapse Uncertainty (β_{TOT})	$ACMR_{10\%}$	$ACMR_{20\%}$
Model	**Test Data**	**Design Requirement**			
Good	Good	Good	0.525	1.960	1.56
		Fair	0.600	2.160	1.66
	Fair	Good	0.600	2.160	1.66
		Fair	0.675	2.380	1.76
Fair	Good	Good	0.600	2.160	1.66
		Fair	0.675	2.380	1.76
	Fair	Good	0.675	2.380	1.76
		Fair	0.725	2.530	1.84

Note: For conservative results, record-to-record uncertainty was rated as poor for all cases of total system collapse uncertainty.

As can be seen, β_{TOT} ranged between 0.525 and 0.725. The *ACMR20%* was 1.84. Since *ACMR* of the structure was 2.2 which was larger than 1.84, this structure was deemed acceptable per FEMA P695.

The fragility curves computed from the IDA results are shown in Figure 6.7. As can be seen, collapse probability for the MCE ground motions falls below the generally acceptable value of 10%. The results indicated that the story drifts reached between 6%-7% before the collapse occurred. The failure pattern was typically the fracture of a set of BRBs quickly followed by excessive rotation of the plastic hinges in the columns. For the columns, the critical plastic hinges were mainly located at the bases except in a few ground motions where they were located elsewhere. At 2/3MCE level (0.64g), there were 97%, 50%, 12%, 3% and 1% probability of maximum interstory drift response being greater than 1%, 2%, 3%, 4% and 6%, respectively. At MCE level (0.96g) there was 100%, 96%, 52%, 30% and 16% probability of a maximum interstory drift response being greater than 1%, 2%, 3%, 4% and 6%, respectively. In summary, for 2/3MCE and MCE levels, the probability of maximum interstory drift greater than 2% and 3% was approximately 50%. In other words, there was approximately 50% probability that the interstory drift will not exceed the target values of 2% and 3% for 2/3MCE and MCE levels, respectively. Regarding collapse, it was found that there was only 6.5% probability of collapse for the MCE level, and almost 0% probability of collapse for the 2/3MCE level.

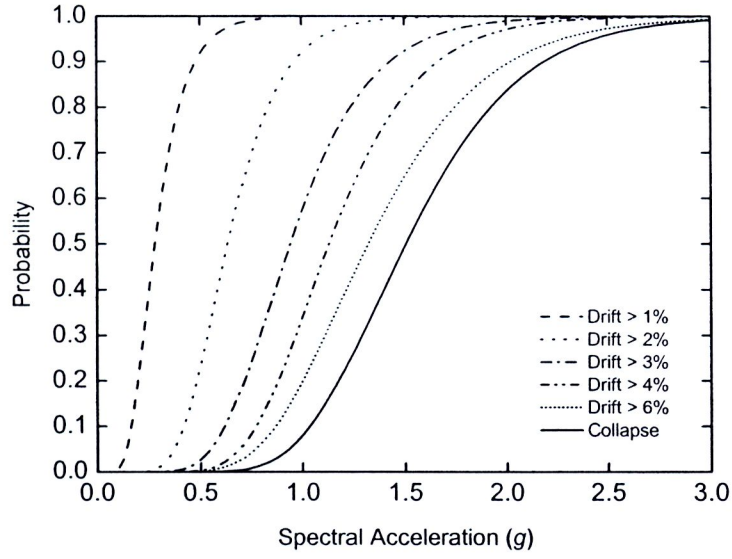

Figure 6.7 Fragility Curve

6.3 Performance Sensitivity

From nonlinear analyses, it was found that the structure lost the ability to resist lateral forces after a set of BRBs fracture as indicated previously. It can be summarized that the deformation capacity of BRBs is the key parameter that governs the structural system ductility. The fragility curves described earlier were computed based on 4% maximum core strain for the BRBs. To analyze the influence of BRB deformation capacity on the overall performance of the system, BRKB-TMF using BRBs with 2 values of maximum core strain limit were examined. The IDA were repeated using 3% and 5% maximum core strain, and the resulting fragility curves are as shown in Figures 6.8 to 6.9.

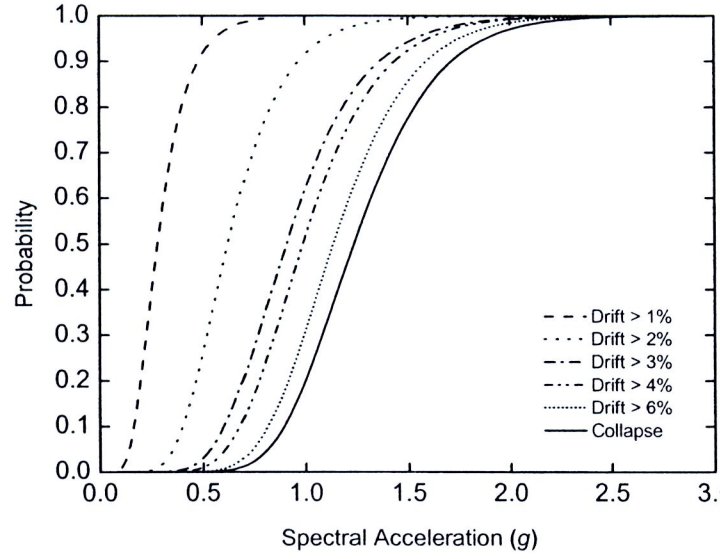

Figure 6.8 Fragility Curves for BRKB-TMF with 3% Maximum BRB Core Strain

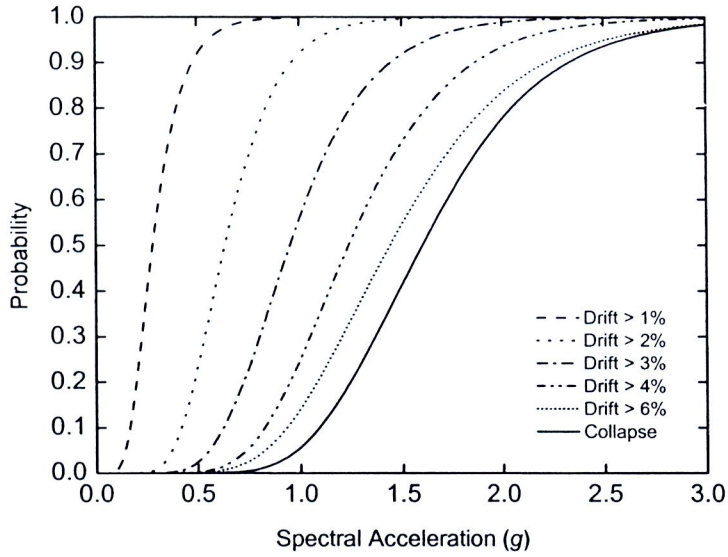

Figure 6.9 Fragility Curves for BRKB-TMF with 5% Maximum BRB Core Strain

As expected, large BRB deformation capacity decreases probability of collapse for a given ground motion intensity. It can also be observed that for the fragility curves of the 3% core strain case, the fragility curves are closely spaced for the drifts beyond 3%. This implies that the deformation tends to increase rapidly towards collapse once the drift passes 3%. On the other hand, fragility curves for the case of 5% core strain limit are closely spaced only for drifts greater than 4%. These drift thresholds depend on the core strain limits of BRBs. Using the approximate equation for plastic deformation of BRBs (Equation 3-1), the relationship between plastic drift ratios and strain demands can be computed as listed in Table 6.3. As can be seen, 3% strain corresponds to the drift of 3% and 5% strain corresponds to the drift of approximately 4%. The drift thresholds can be approximated fairly well using the approximate equation.

Table 6.3 Core Strain Demand Related to Story Drift

Target Drift Ratio θ_u (%)	Yield Drift Ratio θ_y (%)	Inelastic Drift Ratio θ_p (%)	Plastic Strain Demand (%)
1	0.75	0.25	0.3
2	0.75	1.25	1.4
3	0.75	2.25	2.6
4	0.75	3.25	3.7
5	0.75	4.25	4.9
6	0.75	5.25	6.0

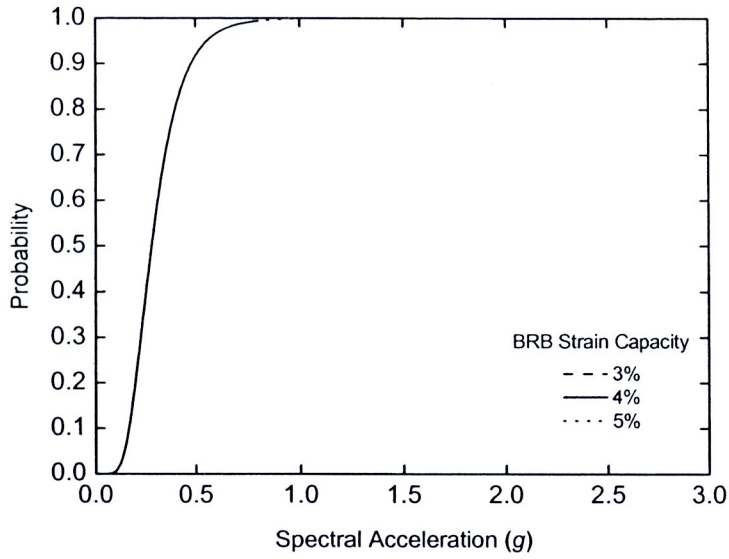

(a) 1% Drift Response

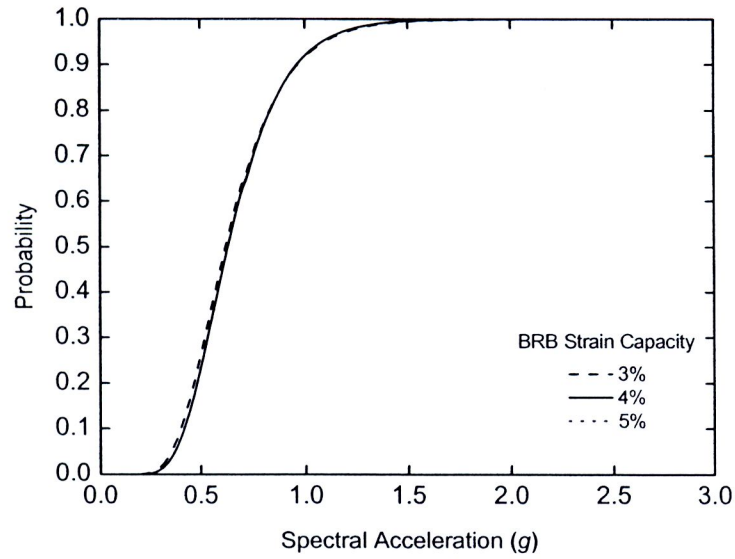

(b) 2% Drift Response

Figure 6.10 Response Sensitivity based on BRB Strain Capacity

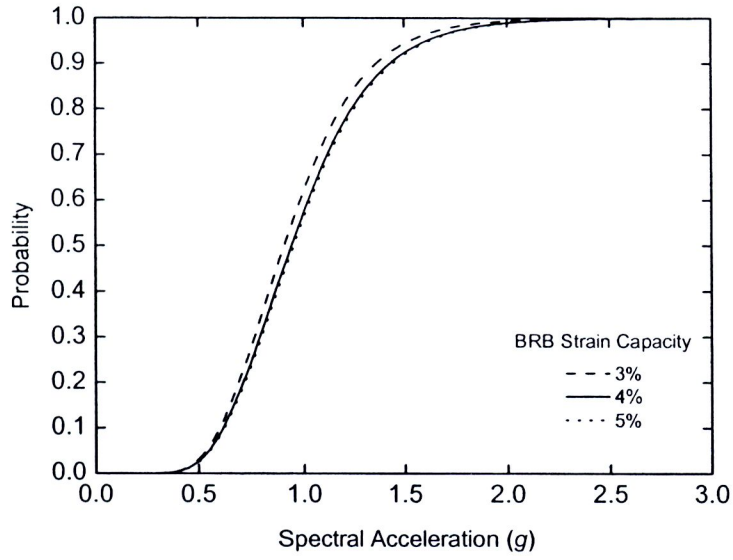

(c) 3% Drift Response

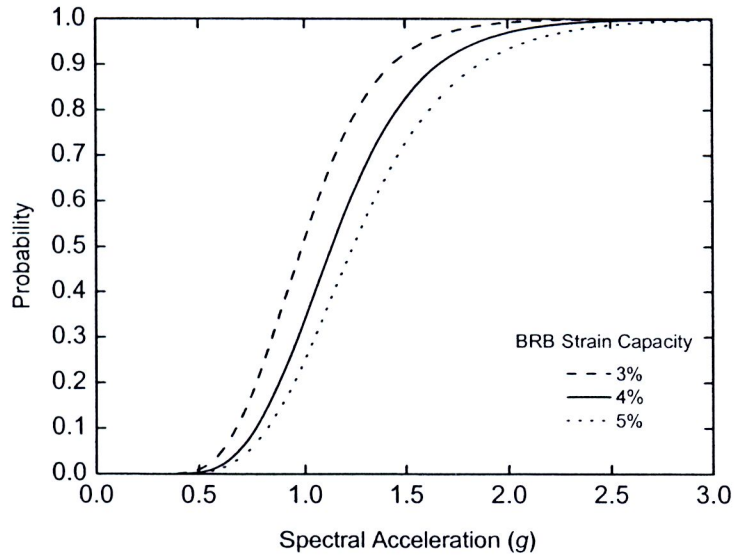

(d) 4% Drift Response

Figure 6.10 Response Sensitivity based on BRB Strain Capacity (Continued)

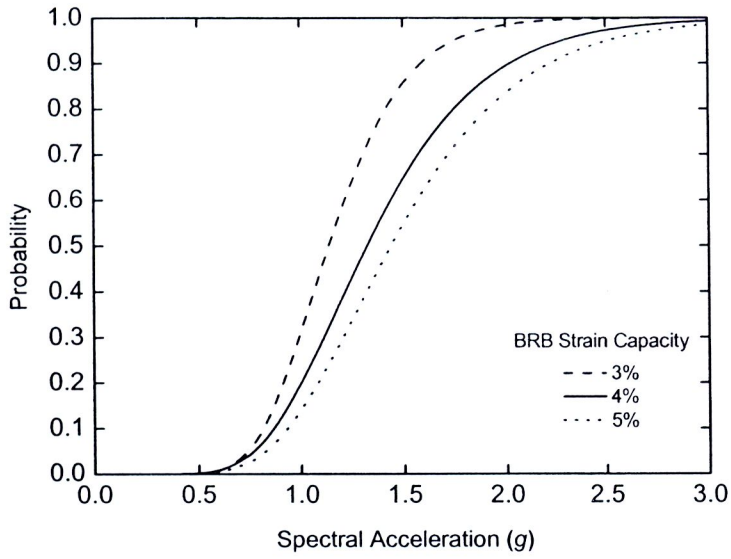

(e) 6% Drift Response

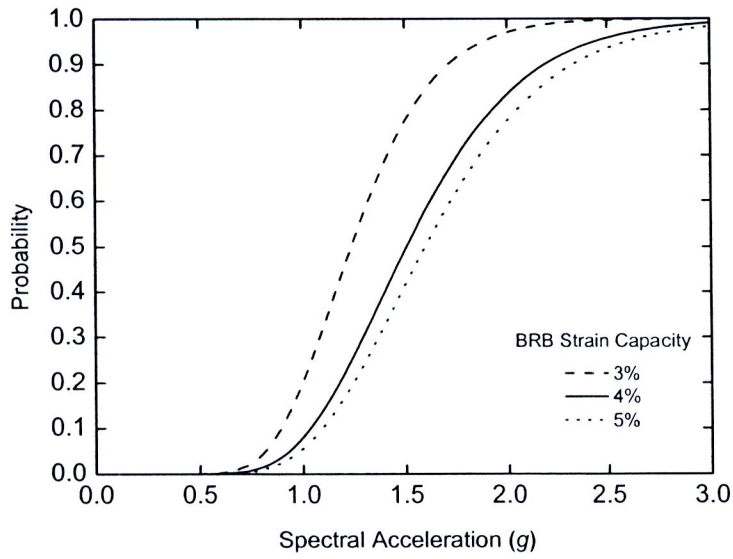

(f) Collapse Level

Figure 6.10 Response Sensitivity based on BRB Strain Capacity (Continued)

The fragility curves for the 3%, 4%, and 5% BRB strain limits are shown for different drift levels in Figure 6.10. At 1% and 2% drift ratios, the approximate plastic strain values in the BRB was 0.3% and 1.4% which were lower than the strain limits for all 3 cases. Therefore, brace fracture should not be found in any of these cases. Hence, the fragility curves appear to be approximately the same in this case. At 3% drift ratio (Figure 6.10c), a slight difference can be observed. At this level, plastic strain demand of BRB is approximately to 2.6% which is almost the same as the 3% strain capacity. Hence, the drift tends to be larger for a given level of ground motion intensity for the case of 3% strain limit. The fragility curves for the 4% and 5% strain limits are approximately the same because fracture was not expected for these strain limits. For all

the remaining drift ratios, including collapse (Figure 6.10d, 6.10e, and 6.10f) the fragility curves for the 3%, 4%, and 5% strain limits are distinctively different from each other. Increasing strain capacity gives better structural response. In terms of the probability of collapse (Figure 6.10f), the differences in the response were largest for the case of 3% and 4% core strain limits. The differences were minor for the case of 4% and 5% core strain limits. This was because when the BRBs could deform more than 4%, the response started to be governed by failure of other components such as columns and top chords of the truss. Therefore, increasing strain capacity of BRBs more than 4% will not significantly improve the system performance. The 4% strain capacity appears to be optimum. This 4% strain capacity is certainly achievable within current technology.